Baghdad Science Journal

Volume 22 | Issue 7 Article 9

7-16-2025

Synthesis and Characterization of CaxNi1-xCr_2O_4 Compound and Studying the effect of the Dopant on its Structural and Optical Properties

Weaam Abdulkader Akkad
Department of Chemistry, Faculty of Science, Al-Baath University, Homs, Syria, weaam.akkad@gmail.com

Ibrahim Ismail
Department of Chemistry, Faculty of Science, Al-Baath University, Homs, Syria,
ibrahemismail186@gmail.com

Adnan Kodala
Department of Chemistry, Faculty of Science, Al-Baath University, Homs, Syria, adn.kod@gmail.com

How to Cite this Article

Akkad, Weaam Abdulkader; Ismail, Ibrahim; and Kodala, Adnan (2025) "Synthesis and Characterization of CaxNi1-xCr_2O_4 Compound and Studying the effect of the Dopant on its Structural and Optical Properties,"
Baghdad Science Journal: Vol. 22: Iss. 7, Article 9.
DOI: https://doi.org/10.21123/2411-7986.4989

BAGHDAD SCIENCE JOURNAL 2025;22(7):2230–2238

RESEARCH ARTICLE

Synthesis and Characterization of $Ca_xNi_{1-x}Cr_2O_4$ Compound and Studying the effect of the Dopant on its Structural and Optical Properties

Weaam Abdulkader Akkad *, **Ibrahim Ismail**, **Adnan Kodala**

Department of Chemistry, Faculty of Science, Al-Baath University, Homs, Syria

ABSTRACT

$Ca_{0.07}Ni_{0.93}Cr_2O_4$ was synthesized using solid-state method at 1000˚C for 6h. Structural properties were studied by using X-ray diffraction and compared with Nickel Chromite compound ($NiCr_2O_4$) which was prepared at the same temperature. XRD patterns showed that Nickel Chromite compound crystallized according to the cubic pattern of the spinel structure. The value of its crystal lattice constant is a = 8.2449 Å. After doping the Nickel Chromite with Calcium, the compound remained maintaining its crystalline structure without any change in the crystal structure, the value of the crystal lattice constant was a = 8.2695 Å , that is slightly larger than its in Nickel Chromite, which was accompanied by an increase in the crystal cell and crystallization size due to the slight increase in the ionomer radii of the two elements. The experimental results were confirmed by using FTIR spectrums, which supported the formation of mixed oxide, and consistent with the results of XRD and SEM. Finally, the effect of this doping on the optical properties was studied,which showed that the value of the energy gap in the Calcium-doped Nickel Chromite compound increases slightly compared to the pure Nickel Chromite compound indicates that the prepared $Ca_{0.07}Ni_{0.93}Cr_2O_4$ compound may be a promising compound as a semiconductor, which makes it preferred in many optics and electronics.

Keywords: Band gap, Optical properties, Solar cells, Spinel structure, Structural properties

Introduction

The study of the development and modernization of various environmentally friendly devices, such as solar cells, batteries, mobile phones, and plasma screens, is the spot light of much scientific research recently, in order to keep pace with the tremendous industrial development witnessed by the modern technological world and to meet different needs in various fields due to the scarcity of fossil fuels. Among these researches, semiconductor metal oxide nanoparticles have received great attention because they are inspiring and have high-performance materials due to their new properties.[1] Spinel-type nanostructures are mixed oxides with general formula (AB_2O_4) where A is a divalent metal B is trivalent. They have been studied due to their excellent properties, such as electrical, thermal, optical, magnetic, and chemical properties.[2] These oxides are characterized by their high thermal stability, resistance to corrosion, catalytic activity, and distinctive optical and magnetic properties.[3,4] In particular, the nickel chromite compound has been studied and its optical bandgap has been calculated in several papers to be 1.7 eV, indicating that $NiCr_2O_4$ nanoparticles are a semiconductor material and can be used in electrical and optoelectronic devices. Many studies have shown that the most widely used methods for preparing these mixed oxides are the solid-state method, the sol-gel method, pyrolysis, the microwave method, co-precipitation, and the hydrothermal method.[5,6] In this research, the solid-state method has been

Received 30 January 2024; revised 12 August 2024; accepted 14 August 2024.
Available online 16 July 2025

* Corresponding author.
E-mail addresses: weaam.akkad@gmail.com (W. A. Akkad), ibrahemismail186@gmail.com (I. Ismail), adn.kod@gmail.com (A. Kodala).

https://doi.org/10.21123/2411-7986.4989

followed[6,7] which relies on the use of oxides, nitrates, or carbonates as raw materials in the preparation process is distinguished by the fact that it enables us to obtain high-purity crystalline compounds for the prepared compound due to starting from primary compounds that do not contain impurities from different materials in the composition. In addition, the resulting crystals are relatively large in size compared to crystals prepared for the same compound using other methods, such as the Sol-Gel method and the co-precipitation method. In addition, this method does not give any secondary products, as is the case with the rest of the methods used, and this makes it easier to read the XRD pattern because the percentage of the selected alloy is very small.[7,8] Therefore, the aim of this research is to study the effect of mixing nickel chromite[9] with calcium oxide due to the close radius of the ionic elements and then study the effect of adding calcium on the structural and optical properties of the prepared compounds.[10–12]

Materials and methods

Each of the following oxides was used as starting materials in synthesis (NiO-Qualikems 70%) – (Cr_2O_3 General Purpose reagent – (CaO Riedel-de Haën 96%).

The previously mentioned materials were used for the synthesis, and the molar ratio 1:1 was adopted to prepare the nickel chromite compound according to the following reaction:

$$NiO + Cr_2O_3 \xrightarrow{\Delta} NiCr_2O_4$$

Then, calcium oxide was replaced by nickel in a ratio x = 0.07 in position A of the spinel structure AB_2O_4 according to the following reaction:

$$_{0.07}CaO + _{0.93}NiO + Cr_2O_3 \xrightarrow{\Delta} Ca_{0.07}Ni_{0.93}Cr_2O_4$$

Weighs 0.01 mol of the raw materials were taken and weighed on a scale accurately 0.0001 gr, then milled using an agate mortar, and the materials were mixed using volatile solvents such as acetone three times in a row in order to help mix and achieve the smoothest possible homogeneity. The samples were dried in an electric dryer for one hour, milled again to ensure complete homogeneity, and then placed in heat-resistant ceramic crucibles in a (CARBOLITE CWF 1200) electric furnace at 1000°C for 6 hours. X-ray diffraction patterns of the resulting samples were drawn using a diffractometer (PW-1840) (CoKα) at a wavelength $\lambda = 1.78897$ Å). Infrared spectra (Jascoo-FTIR) was used for prepared samples in the range of 4000 to 400 cm^{-1}). The Morphology of the obtained spinel oxides was showed using a Qaunta 200 scanning electron microscope (SEM). Finally, the effect of this dopant on the optical properties was studied by using the DRS device (Diffuse reflectance spectroscopy) to determine the effect of this dopant on the band gap.

Results and discussion

X-ray diffraction (XRD) analysis

X-ray diffraction spectroscopy is one of the most important techniques used in characterizing crystalline materials. It enables us to identify Miller's evidence, deduce the crystallization pattern of the compound studied, find the dimensions of the crystal cell, the basic principles of the crystal lattice (crystal lattice constants) and also calculate the size of the basic crystal cell, as it gives information about the purity of the material and the presence of impurities and other phases in the crystal lattice.

Fig. 1 shows the X-ray diffraction pattern for Nickel Chromite and Calcium-doped Nickel Chromite compounds:

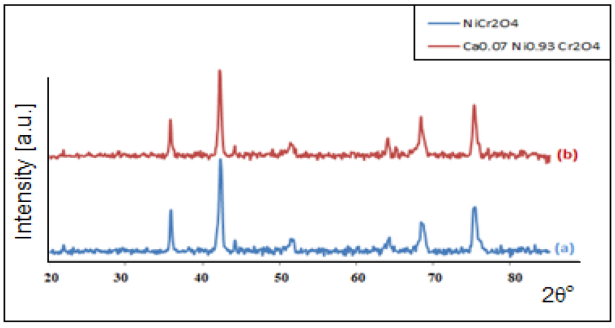

Fig. 1. XRD pattern for (a) Nickel Chromite (b) Calcium-doped Nickel Chromite compounds prepared by solid-state method at 1000°C for 6 h.

By matching the resulting peaks in Fig. 1 with the ref card number [JCPDS No: 231271] shown in Table 1. as follows:

Table 1. Reference card for Nickel Chromite with a cubic structure.

2θ	I%	hkl	2θ	I%	hkl
21.036	20	111	50.94	20	400
35.302	55	220	63.494	20	422
41.755	100	311	67.836	35	511
43.574	5	222	74.842	50	440

Cubic a = 8.316 (Å) V = 575.10($Å^3$) S.G: Fd3m(227)

It turns out that all the peaks in Fig. 1 belong to Face Centered Cubic (FCC) structure with Fd3m space group of symmetry.[13] The values of the diffraction angles of the prepared Nickel Chromite compound, the distance between the crystal centers and the

Table 2. Values of (2θ, d, hkl, a) for Nickel Chromite compound prepared by solid-state method at 1000°C for 6 h: $Q = [(10^4/d^2)/148] = h^2 + k^2 + l^2$.

2θ	I%	d_{exp}(Å)	d_{card}(Å)	$10^4/d^2$	$h^2+k^2+l^2$	hkl	a (Å)
21.75	8.04	4.7410	4.9000	444.8828	3	111	8.21179
35.75	47.28	2.9141	2.9499	1177.5104	8	220	8.24257
42.25	100	2.4818	2.5099	1623.4268	11	311	8.23151
44.15	12.39	2.3800	2.4099	1765.2798	12	222	8.24487
51.65	14.86	2.0533	2.0800	2371.7956	16	400	8.21336
64.05	10.37	1.6867	1.6999	3514.6292	24	422	8.26353
68.45	29.19	1.5903	1.6030	3953.7825	27	511	8.26371
75.25	47.16	1.4651	1.4719	4658.1357	32	440	8.28836

$\bar{a} = 8.2449$ Å.

Miller clues were calculated. To verify the validity of this comparison a trial-and-error method was followed as shown in the Table 2.

From Table 2 and evaluating Miller's evidence hkl, it is noted that the following condition applies to it:

$$h + k = 2n \quad h + l = 2n \quad k + l = 2n$$

This indicates that all vertices belong to a cubic structure according to pattern FCC. The basic unit cell volume was calculated from Eq. (1):[14]

$$V = a^3 \tag{1}$$

Pycknometer used to determine the density of solid compound that does not dissolve in water. Weigh of pycknometer must be measured empty (m_0) and with solid compound ($m_0 + m_s$); then add water and determine the total weight to calculate m_{H_2O} from Eqs. (2) and (3):

$$m_{tot} = m_0 + m_s + m'_{H_2O} \tag{2}$$

$$m'_{H_2O} = m_{tot} - (m_0 + m_s) \tag{3}$$

The volume of added water V'_{H_2O} can be obtained from Eq. (4):

$$V'_{H_2O} = \frac{m'_{H_2O}}{\rho_{H_2O}} \tag{4}$$

The volume of measured solid compound (V_s) is determined from Eq. (5):

$$V_s = V - V'_{H_2O} = \frac{m_{H_2O}}{\rho_{H_2O}} - \frac{m'_{H_2O}}{\rho'_{H_2O}} \tag{5}$$

Finally, density of solid compound ρ_s can be calculated from Eq. (6):

$$\rho_s = \frac{m_s}{V_s} \tag{6}$$

By knowing the molecular weight of the $NiCr_2O_4$ compound and after calculating its experimental density using a density flask pycknometer, the number of formulas Z in one cell is calculated and it is converted to the nearest integer using the Eq. (7):

$$\rho = \frac{MZ}{N_a V} \tag{7}$$

Where M molecular weight of the material, N_a Avogadro number, and V basic unit cell volume, it was found that:

$$Z = \frac{\rho N_a . V}{M}$$

$$= \frac{5.241 \ \left(\frac{gr}{cm^3}\right) \times 6.022 \times 10^{23} (mol^{-1}) \times 560.4886 \times 10^{-24} (cm^3)}{226.69 \left(\frac{gr}{mol}\right)}$$

$$= 7.803498157 \cong 8$$

Then the general formula for the basic cell content can be written as follows $Ni_8Cr_{16}O_{32}$. That is, one cell contains eight nickel atoms, sixteen chromium atoms, and thirty-two oxygen atoms. By replacing the value of Z = 8 as an integer in the previous equation to get the theoretical density value as is evident in the Eq. (8). The calculated value was very close to the experimental value, which proves the accuracy of the theoretical calculations and the accuracy of choosing the basic unit cell.

$$\rho_T = 5.372 \ gr/cm^3 \tag{8}$$

The crystallization volume was calculated from Debye-Scherer Formula[12,13] Eq. (9):

$$L = \frac{k \lambda}{\beta \cos\theta} \tag{9}$$

where L is grain size (nm), k is a constant equal to 0.9 λ is wavelength of the XRD, θ is Bragg's diffraction angle and β is full width at half maximum of the peak (radians).

The results obtained are shown in Table 3:

Table 3. Structural characteristics of the $NiCr_2O_4$ compound prepared by solid-state method at 1000°C for 6 h.

a (Å)	V (Å)^3	ρ_E	Z	ρ_T	L (nm)
8.2449	560.4886	5.241	8	5.372	23.18[18]

Comparing the crystallization volume calculated from Debye-Scherer Formula, the value of the crystallization volume reached 23.18 nm, which is very close to the value calculated according to ref, [14] which amounted to 24 nm. After that, the XRD diffraction pattern for Calcium -doped Nickel Chromite with a ratio of x = 0.07 at 1000°C and was as follows in Fig. 1b. The values of the diffraction angles of the Calcium-doped Nickel Chromite compound, the distance between the crystal planes, and Miller's evidence were calculated. [15] To verify the validity of this comparison a trial-and-error method was followed as in Table 4.

The number of formulas in a single crystalline cell Z was calculated by Eq. (7):

$$Z = \frac{5.3101\ \left(\frac{gr}{cm^3}\right) \times\ 6.022\ \times 10^{23}\left(mol^{-1}\right) \times 565.516\ \times 10^{-24}\left(cm^3\right)}{225.3801\ \left(\frac{gr}{mol}\right)}$$

$$= 8.0236648\ \cong\ 8$$

By replacing the value of Z as an integer in Eq. (7), theoretical density value was determined as is evident in the Eq. (10), and the calculated value was very close to the experimental value, which proves the accuracy of the theoretical calculations and the accuracy of choosing the basic unit cell.

$$\rho_T = 5.2944\ gr/cm^3 \qquad (10)$$

Finally, the crystallization volume and the values of some structural properties of the $Ca_{0.07}Ni_{0.093}Cr_2O_4$ compound prepared by the solid-state method and incinerated at 1000°C were calculated, and the results were arranged in Table 5.

Table 4. Values of (2θ, d, hkl, a) for Calcium-doped Nickel Chromite prepared by solid-state method at 1000°C for 6 h: Q = $[(10^4/d^2)/148] = h^2 + k^2 + l^2$.

2θ	I%	d_{exp}(Å)	$10^4/d^2$	$h^2+k^2+l^2$	hkl	a (Å)
21.55	1.24	4.7845	436.844	3	111	8.2870
35.65	40.29	2.9220	1171.791	8	220	8.2649
42.15	100	2.4875	1614.390	11	311	8.2501
44.05	9.77	2.3852	1753.432	12	222	8.2626
51.45	12.57	2.0607	2353.794	16	400	8.2431
63.95	19.78	1.6891	3498.177	24	422	8.2750
68.25	43.36	1.5944	3933.228	27	511	8.2849
75.25	55.35	1.4651	4650.046	32	440	8.2883

$\bar{a} = 8.2695$.

Table 5. Structural characteristics for calcium-doped nickel chromite prepared by solid-state method at 1000°C.

a (Å)	V (Å)^3	ρ_E	Z	ρ_T	L (nm)
8.2695	565.516	5.3101	8	5.2944	24.35

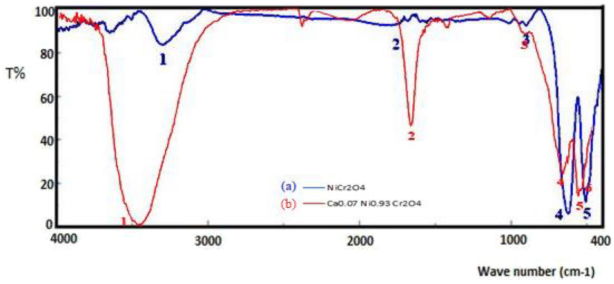

Fig. 2. FTIR spectra of a. Nickel Chromite - b. Calcium-doped Nickel chromite prepared by solid-state method at 1000°C for 6 h.

All the peaks are identical in both compounds and they belong to a cubic structure FCC with Fd3m symmetry pattern. That is, when replacing the nickel element $r_{Ni^{2+}} = 0.069$ nm with the calcium element with a radius $r_{Ca^{2+}} = 0.100$ nm, No changes were observed in the crystalline structure of nickel chromite due to the close radius between the two elements and the low percentage of doping as well, noting an increase in the intensity of the peaks when calcium is added, which indicates an increase in the size of crystallization due to the increase in the values of the diffraction angles when doping in small percentages.

Fourier transform infrared (FTIR) spectroscopy

The structure of the compounds prepared by the aforementioned ceramic method and within the same molar ratio was also studied using infrared spectroscopy, and it was noted that the obtained results were consistent with the results of that agrees with the ref. [16]

Fig. 2a, shows the variation of the absorption bands and the wavenumbers [16,17] for $NiCr_2O_4$. Sequentially absorptions at 623.85 and 505.258 cm^{-1} confirm the formation of M-O (Cr-O and Ni-O) bonds, which is due to the vibrations of the bonds inside the octahedrons and tetrahedrons, respectively. These peaks are due to the vibrations of the A-O and B-O bonds within the tetrahedrons and octahedrons, respectively, within the spinel structure, and this confirms the formation of the compound; which had agreed with the ref. [14]

A single absorption band at around 893.59 cm^{-1} indicated the metal-metal (Ni-Cr) vibrational frequencies1. [17] The OH stretching and bending modes of adsorbed water molecules are shown at 3297.68 and 1790.58 cm^{-1}, respectively.

Table 6. Shows the absorption bands in the previous spectrum and the wavenumbers[17] for each:

Table 6. Absorption bands and wavenumbers of the infrared spectrum of Nickel Chromite prepared by the ceramic method at 1000°C for 6 h.

Absorption band No.	υ (cm^{-1})	Vibration pattern
1	3297.68	O-H bond stretching
2	1790.58	O-H bending vibration
3	893.59	Ni-Cr vibrational frequencies
4	623.856	Cr-O bond stretching
5	505.258	Ni-O bond stretching

Sequentially absorptions in Fig. 2b. at 624.961 and 508.258 cm^{-1} confirm the formation of M-O (Cr-O and Ni-O) bonds which is due to the vibrations of the bonds inside the octahedrons and tetrahedrons respectively. These bands belong to normal spinel peaks as in $NiCr_2O_4$ spectrum.

The absorption band 438.73 cm^{-1} indicated the M-O (Ca-O) vibrational frequency. The OH stretching and bending modes of adsorbed water molecules are shown at 3439.42 and 1635.34 cm^{-1}, respectively. Table 7 shows the absorption bands in the previous spectrum and the wave numbers for each of them:

Table 7. Absorption bands and wavenumbers of the infrared spectrum of Calcium-doped Nickel Chromite prepared by the ceramic method at 1000°C for 6 h.

Absorption band No.	υ (cm^{-1})	Vibration pattern
1	3439.42	O-H bond stretching
2	1635.34	O-H bending vibration
3	900.597	Ni-Cr vibrational frequencies
4	624.961	Cr-O bond stretching
5	508.258	Ni-O bond stretching
6	438.726	Ca-O bond stretching

By comparing the values of the absorption bands in Fig. 1, a slight shift of some peaks towards larger values was observed as a result of the addition of calcium oxide. This indicates an increase in the size of crystallization, as shown by the XRD diffraction patterns of samples with the appearance of a new absorption peak due to Ca-O bond stretching.

It was noted that there was a large degree of similarity in peaks between the two spectra, as a result of the small percentage of doping used.

Scanning electron microscope SEM

A scanning electron microscope was used to characterize the surface morphology and particle size distribution. Electron microscope images are shown in Fig. 3 of two samples of pure Nickel Chromite and Calcium-doped Nickel Chromite prepared by solid-state method at 1000°C. Most of the particles appeared regular in the micrograph, with an increase in crystallite size observed in the Calcium-containing

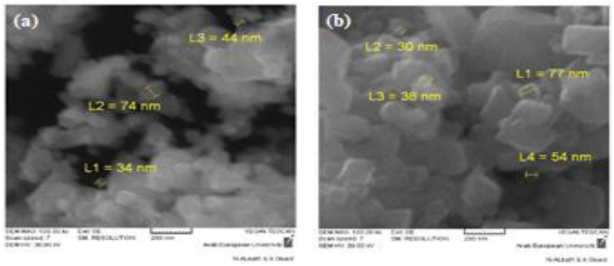

Fig. 3. SEM image of (a) $NiCr_2O_4$ (b) $Ca_{0.07}Ni_{0.93}Cr_2O_4$ nanoparticles prepared by solid-state method at 1000 °C for 6 h.

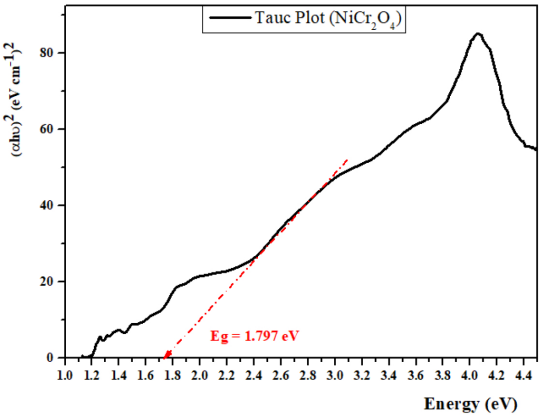

Fig. 4. Band gap diagram of $NiCr_2O_4$ nanoparticles prepared by solid-state method at 1000°C for 6 h.

sample, which is consistent with the XRD results. The particle size ranged between 30–77 nm.

Band-gap analysis

The band gap is an important parameter for a semiconductor, which determines its application capabilities in optoelectronics. A semiconductor with a suitable bandgap can absorb a lot of light in solar cells, but as the value of the bandgap increases greatly, it becomes difficult to absorb light. Therefore, the optical band gap of a material is an important parameter by which the optical and electrical properties of materials are determined for use in many applications. For direct band gap determination, a plot of $(\alpha h\upsilon)^2$ versus energy[18,19] is presented in Figs. 4 and 5. according to Tauc-Plot[20] which shown in Eq. (11):

$$(\alpha h\nu)^n = k(h\nu - E_g) \quad (11)$$

Where n = 2 for direct band gap; and n = ½ for indirect band gap. When the value is replaced with 2, a linear portion appears in the graph Which will not appear if the substance has indirect transmission unless it is n = ½. Band gap value was obtained

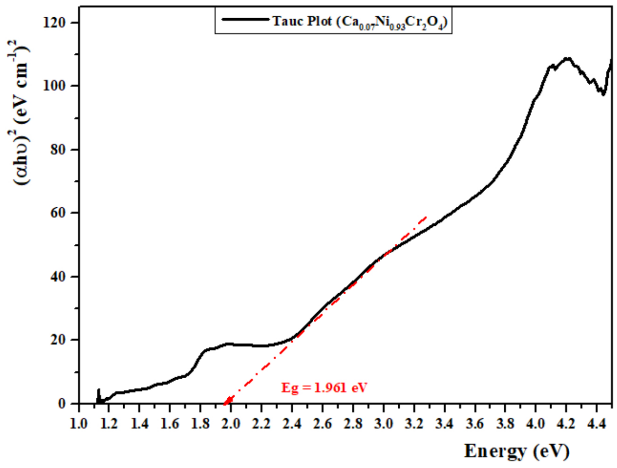

Fig. 5. Band gap diagram of $Ca_{0.07}Ni_{0.93}Cr_2O_4$ nanoparticles prepared by solid-state method at 1000 °C for 6 h.

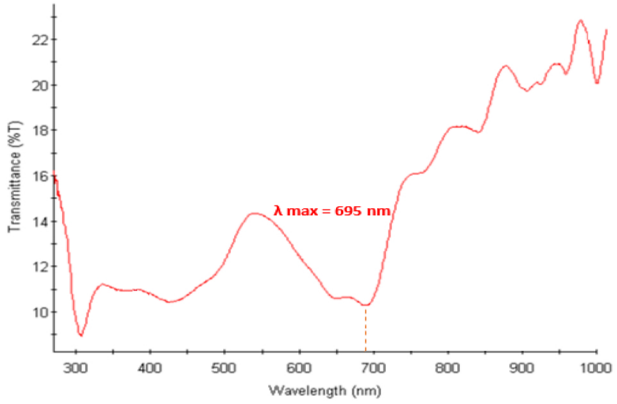

Fig. 6. DRS spectra for $NiCr_2O_4$ nanoparticles prepared by solid-state method at 1000 °C for 6 h.

by extrapolating the straight portion of the graph on the hυ axis at $(\alpha h\upsilon)^2 = 0$.[21,22] When the slope of the line segment is drawn and projected onto the axis X, the value of Eg is obtained for these compounds.

Figs. 4 and 5, show that the value of the band gap of the prepared Nickel Chromite compound is 1.797 eV while its value was in Calcium-doped Nickel Chromite 1.961 eV. This increase is due to the addition of Calcium, because Calcium Chromite has a larger energy gap than Nickel Chromite. To confirm the previous results, we studied the Diffuse Reflection Spectra (DRS) of the prepared compounds Figs. 6 and 7.

The energy gap and wavelength of the absorbed rays were calculated using DRS spectrums for the prepared compounds as shown in Table 8.

As the ionic radius of the substituted element increased, the polarity increased, and the bonds became weaker, thus the charge transfer was less, therefore

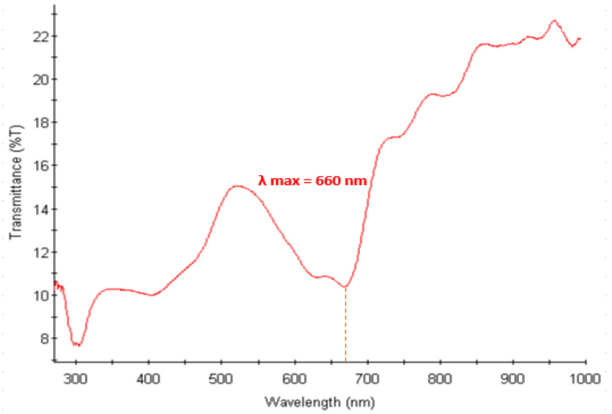

Fig. 7. DRS spectra for $Ca_{0.07}Ni_{0.93}Cr_2O_4$ nanoparticles prepared by solid-state method at 1000 °C for 6 h.

Table 8. Energy gap and wavelength of absorbed rays using DRS spectrums for prepared compounds.

Compound Formula	Eg (eV)	λ (nm)	Type of light rays absorbed
$NiCr_2O_4$	1.784	695	Vis – red
$Ca_{0.07}Ni_{0.93}Cr_2O_4$	1.878	660	Vis – red

they showed absorption at lower wavelengths. We conclude from the above that the prepared compounds are semiconductors and promising for use in photovoltaic cells due to their ability to absorb light rays, even in the infrared range.

Conclusion

Nickel Chromite and Calcium doped Nickel Chromite were prepared by the solid-state method at 1000°C for 6h based on their primary oxides. Both compounds were crystallized according to a cubic, spinel-type structure FCC and the results were supported by XRD. The value of the crystal lattice constant in each of them was 8.2449–8.2695Å respectively because the ion radius of Calcium is larger than that of Nickel, which is accompanied by an increase in crystalline size and grain size. The formation of the compounds was confirmed by FT-IR due to the appearance of absorption bands between 400–1000 cm^{-1}, the peaks belonging to the bond vibration (M-O) confirmed that they belong to the vibration of bonds within the octahedrons and tetrahedrons formed within the spinel structure and then the band gap in each of them was calculated. It was found that when Calcium ion was added, even in small proportions, it caused an increase in the value of band gap, which indicated it as a semiconductor, which makes it preferred in many optical and electronics applications.

Acknowledgment

The authors are grateful to Dr. Abla Alzoubi the technical team in XRD Lab at Al-Baath University, Homs, Syria for XRD experiments, and Dr. Abdullah Al-Hasan, the Scientific Research Authority in Homs, Syria for his support in this research.

Author's declaration

- Conflicts of Interest: None.
- We hereby all the Figures and Tables in the manuscript are ours. Any Figures and images, that are not ours, have been included with the necessary permission for re-publication, which is attached to the manuscript.
- No animal studies are present in the manuscript.
- No human studies are present in the manuscript.
- Ethical Clearance: The project was approved by the local ethical committee at Al-Baath University.

Author's contribution

W.A. and A.K. worked at conceptualization, methodology, acquisition of data, interpretation, drafting the manuscript, and designing original draft preparation. I.I. worked at visualization, investigation, editing, analysis, revision, and proofreading. All authors agreed upon the final version of the manuscript.

References

1. Ragupathi C, Narayanan S, Tamizhdurai P, Govindasamy M, ALOthman ZA, Al-Anazy MM. Tuning magnetic, electronic, and optical properties of Mn-doped $NiCr_2O_4$ via microwave method. Arab J Chem. 2021 Jul 1;25(7):101275. https://doi.org/10.1016/j.jscs.2021.101275.
2. Shafqat MB, Ali M, Atiq S, Ramay SM, Shaikh HM, Naseem S. Structural, morphological and dielectric investigation of spinel chromite (XCr_2O_4, X = Zn, Mn, Cu & Fe) nanoparticles. J Mater Sci: Mater Electron. 2019 Oct;30(7–8):17623–17629. https://doi.org/10.1007/s10854-019-02111-4.
3. Wang YAT, Yan N, Yan Z, Zhao B, Zhao F. Nanochromates MCr_2O_4 (M = Co, Ni, Cu, Zn): preparation, characterization, and catalytic activity on the thermal decomposition of fine AP and CL-20. ACS Omega. 2019 Dec 26;5(1):327–333. https://doi.org/10.1021/acsomega.9b02742.
4. Ragupathi C, Vijaya JJ, Surendhar P, Kennedy LJ. Comparative investigation of nickel aluminate ($NiAl_2O_4$) nano and microstructures for the structural, optical and catalytic properties, Polyhedron. 2014;72:1–7. https://doi.org/10.1016/j.poly.2014.01.013.
5. Wold A, Dwight K. Solid state chemistry: synthesis, structure, and properties of selected oxides and sulfides. Springer. 1993 Apr 30;(6):70–88. http://dx.doi.org/10.5772/intechopen.93337.
6. Cherosov M, Batulin R, Kiiamov A, Rogov A, Vakhitov I, Gabadullin D, *et al.* Interrelation between the Solid-State Synthesis Conditions and Magnetic Properties of the $NiCr_2O_4$ Spinel. Magnetochemistry. 2022 Dec 30;9(1):13. https://doi.org/10.3390/magnetochemistry9010013.
7. Iskrina AV, Bobrov AV, Spivak AV. Role of Mn doping on magnetic properties of multiferroic $NiCr_2O_4$ nanoparticles. Elements (Que). 2022 Apr;60(4):311–24. https://doi.org/10.1134/S0016702922040024.
8. Hamad IA, Khaleel RI, Raoof AM. Structural and optical properties for nanostructure (Ag_2O/Si & Psi) films for photodetector applications. Baghdad Sci J. 2019 Jul 2;16(4):1036–1042. http://dx.doi.org/10.21123/bsj.2019.16.4(Suppl.).1036.
9. Muhammed SA, Abbas NK. Synthesis and investigation of structural and optical properties of CdO: Ag nanoparticles of various concentrations. Baghdad Sci J. 2023;20(5 Suppl.):17623–17629. https://dx.doi.org/10.21123/bsj.2023.7292.
10. Javed M, Khan AA, Kazmi J, Mohamed MA, Khan MN, Hussain M, *et al.* Dielectric relaxation and small polaron hopping transport in sol-gel-derived $NiCr_2O_4$ spinel chromite. Mater Res Bull. 2021 Jun 1;138:111242. https://doi.org/10.1016/j.materresbull.2021.111242.
11. Rasool RZ, Nadeem K, Kamran M, Zeb F, Ahmad N, Mumtaz M. Comparison of anomalous magnetic properties of non-collinear $CoCr_2O_4$ and $NiCr_2O_4$ nanoparticles. J Magn Magn Mater. 2020 Nov 15;514:167225. https://doi.org/10.1016/j.jmmm.2020.167225.
12. Hakeem HS, Abbas NK. Preparing and studying structural and optical properties of $Pb_{1-x}Cd_xS$ nanoparticles of solar cells applications. Baghdad Sci J. 2021 Sep 1;18(3):0640–0648. https://doi.org/10.21123/bsj.2021.18.3.0640.
13. Bokuniaeva AO, Vorokh AS. Estimation of particle size using the Debye equation and the Scherrer formula for polyphasic TiO_2 powder. J Phys. 2019;1410(1):012057. https://doi.org/10.1088/1742-6596/1410/1/012057.
14. Enhessari M, Salehabadi A, Khanahmadzadeh S, Arkat K, Nouri J. Modified sol-gel processing of $NiCr_2O_4$ nanoparticles; structural analysis and optical band gap. High Temp Mater Process. 2017 Feb 1;36(2):121–5. https://doi.org/10.1515/htmp-2015-0223.
15. Goga F, Bortnic RA, Avram A, Zagrai M, Barbu Tudoran L, Mereu RA. The effect of Ni^{2+} ions substitution on structural, morphological, and optical properties in $CoCr_2O_4$ matrix as pigments in ceramic glazes. Materials. 2022 Dec 7;15(24):8713. https://doi.org/10.3390/ma15248713.
16. Ragupathi C, Narayanan S, Tamizhdurai P, Sukantha TA, Ramalingam G, Pachamuthu MP, *et al.* Correlation between the particle size, structural and photoluminescence spectra of nano $NiCr_2O_4$ and La doped $NiCr_2O_4$ materials. Vaccine Rep. 2023 Nov 1;9(11):21981. https://doi.org/10.1016/j.heliyon.2023.e21981.
17. Permatasari TW, Wijaya HW, Taufiq A, Dasna IW. The effect of addition Ni^{2+} to Cr_2O_3 and its potential characterization as anode potassium ion battery. Int J Mod Phys Conf Ser 2021;1811(1):012032. https://doi.org/10.1088/1742-6596/1811/1/012032.
18. Jubu PR, Obaseki OS, Ajayi DI, Danladi E, Chahrour KM, Muhammad A, *et al.* Considerations About the Determination of Optical Bandgap from Diffuse Reflectance Spectroscopy Using the Tauc Plot. J Opt. 2024 Feb 24:1–1.
19. Al-Mahamad LL. Analytical study to determine the optical properties of gold nanoparticles in the visible solar spectrum. Vaccine Rep. 2022 Jul 1;8(7):09966. https://doi.org/10.1016/j.heliyon.2022.e09966.

20. Mergen ÖB, Arda E. Determination of optical band gap energies of CS/MWCNT bio-nanocomposites by Tauc and ASF methods. Synth Met. 2020 Nov 1;269:116539. https://doi.org/10.1016/j.synthmet.2020.116539.
21. Johannes AZ, Pingak RK, Bukit M. Tauc Plot Software: Calculating energy gap values of organic materials based on Ultraviolet-Visible absorbance spectrum. IOP Conf Ser Mater Sci Eng. 2020;823(1):012030. http://dx.doi.org/10.1088/1757-899X/823/1/012030.
22. Zhang W, Chai C, Fan Q, Song Y, Yang Y. Direct and quasi-direct band gap silicon allotropes with low energy and strong absorption in the visible for photovoltaic applications. Results Phys. 2020 Sep 1;18:103271. https://doi.org/10.1016/j.rinp.2020.103271.

تحضير وتشخيص مركب $Ca_xNi_{1-x}Cr_2O_4$ ودراسة تأثير هذه الإشابة على خصائصه البنائية والضوئية

وئام عقاد، إبراهيم اسماعيل، عدنان كودلأ

قسم الكيمياء، كلية العلوم، جامعة البعث، حمص، سوريا

الخلاصة

تم في هذا البحث تصنيع مركب $Ca_xNi_{1-x}Cr_2O_4$ النانوي وذلك باستخدام طريقة الاصطناع الصلب حيث 7عند الدرجة. حيث قمنا بدراسة خصائصه البنائية باستخدام مخططات الأشعة السينية. وبعد ذلك تمت مقارنة نتائجه مع مركب كروميت النيكل ($NiCr_2O_4$) المحضر عند نفس درجة الحرارة. أظهرت مخططات الأشعة السينية أن مركب كروميت النيكل تبلور وفق النمط المكعبي متمركز الوجوه لنظام الإسبنيل AB_2O_4 فقد بلغت قيمة ثابت الشبكة البلورية للخلية الأساسية a=8.2449Å وبعد إشابة مركب كروميت النيكل بعنصر الكالسيوم وفق النسبة المذكورة سابقاً بقي المركب محافظاً على بنيته البلورية المكعبية متمركزة الوجوه دون أي تغيير في التركيب البلوري. حيث بلغت قيمة ثابت الشبكة البلورية a =8.2695 Å وهي أكبر بقليل منها في كروميت النيكل والذي رافقه زيادة في الحجم البلوري وحجم التبلور والكثافة التجريبية وذلك بسبب الزيادة الطفيفة في أنصاف الاقطار الأيونية لعنصري النيكل والكالسيوم. قمنا بتأكيد النتائج التجريبية باستخدام مخطط الأشعة تحت الحمراء والتي دعمت تشكل الاكسيد المختلط من خلال تشكل الرابطة M-O-M وهذا ما تطابق مع نتائج الأشعة السينية. وأخيراً قمنا بدراسة تأثير هذه الإشابة الصغيرة على الخصائص الضوئية وذلك باستخدام علاقة Tauc Plot وحساب عرض المجال المحظور للانتقال المباشر وتم رسم المنحنيات البيانية الموافقة والتي أظهرت أن قيمة عرض المجال المحظور في مركب كروميت النيكل المشاب بالكالسيوم أكبر بقليل منها في مركب كروميت النيكل النقي، مما يدل على أن مركب $Ca_xNi_{1-x}Cr_2O_4$ المحضر قد سلك سلوك شبه موصل مما يجعله مفضلاً في كثير من التطبيقات الضوئية والإلكترونيات.

الكلمات المفتاحية: عرض المجال المحظور، خصائص ضوئية، خلايا شمسية، بنية سبانيل، خصائص بنائية.